Numerical Analysis of Conjugate Heat Transfer in Foams

N. Bianco*[1], R. Capuano[1], W. K. S. Chiu[2], S. Cunsolo[1], V. Naso[1] and M. Oliviero[1].
[1] DETEC, Università degli studi Federico II, Napoli, Italy
[2] Department of Mechanical Engineering, University of Connecticut, Storrs, CT, USA
* Piazzale Tecchio, 80 – 80125 – Napoli – Italy – nicola.bianco@unina.it

Abstract: A conjugate conductive-convective-radiative discrete model useful for the study and the simulation of heat transfer in a ceramic or metallic foam is presented. A Generation-based Technique is used for the foam representation, using the Weaire-Phelan structure and heat transfer is studied using the COMSOL® Multiphysics. The computational domain is made up by a single cell and a fictitious inlet region, useful to make negligible the lead effects, is considered. The cell consists of the solid phase and of the fluid. The distribution of the cell surface temperature, velocity and pressure, together with temperature and pressure fields as well as velocity fields in the mid-sections of the cell are presented. Results from these simulations are useful to evaluate heat transfer coefficients to be employed in continuous models of the foam.

Keywords: Ceramics foams, Discrete representation, Conjugate heat transfer, Numerical analysis.

1. Introduction

Ceramic and metallic open cell foams have found a wide variety of applications in heat exchangers, energy absorption, flow diffusion and lightweight optics. Extremely fine-scale open-cell foams are used as high-temperature filters in the chemical industry. Ceramic and metallic foams used in compact heat exchangers increase the heat transfer at the cost of an additional pressure drop. However, their use permits to reduce substantially the physical size of a heat exchanger and, therefore, also the fabrication costs [1, 2].

Thus, an effective heat transfer to fluids can be realized only with a good heat transfer inside the foam itself. As a consequence, design and optimization based on porous media can be obtained only if material thermal behavior can be predicted.

The study of heat transfer inside the porous foam can be carried out by means of simplified models, that consider a continuous representation of the foams. These models use a set of parameters and coefficients derived from the analysis of the corresponding discrete system [3,4] and that can be evaluated in a number of ways, such as experimental data fitting, numerical simulation, literature research.

Lee and Vafai [5] presented an analytical model for the solid and the fluid temperatures in porous media. They identified three regimes, each dominated by one of the three mechanisms: fluid conduction, solid conduction and internal heat transfer between the solid and the fluid. They used the Darcy flow model for the velocity distribution inside the foam. Angirasa [6] reported numerical results for convection heat transfer in fibrous heat dissipators using water as the cooling fluid.

Poulikakos and Renken [7] presented numerical simulation results for a channel filled with a fluid-saturated porous medium. They showed that the Darcy flow model underpredicted the heat transfer rate. Poulikakos and Kazmierczak [8] studied forced convection in a duct partially filled with a porous material represented as a continuous shape characterized by a set of average parameters and coefficients evaluated by a previous discrete analysis. Seyf and Layeghi [9] analyzed the convective heat transfer from elliptic pin fin heat sink with and without metal foam insert using a continuous representation of the foam.

Usually, the continuous representation provides a computationally light and stable analysis of heat transfer and any kinds of geometry can be easily handled. On the other hand, the smaller the typical scale of the fields the larger the inaccuracy in the material behavior due to the continuous representation.

For this reason, many researchers have focused the attention on the feasibility to investigate heat transfer in metallic and ceramic foams using a numerical procedure characterized by a discrete representation of the foam achievable either with well known

models (Generation-based Technique) or with a tomography scan of the foam (Imaging-based Technique).

The Generation-based Technique relies on the use of representative models, such as the Kelvin structure or the Weaire-Phelan structure.

The Imaging-based Technique uses a tomography scan of the foam with a subsequent thresholding and 3-D reconstruction of the image [10].

Boomsa and Poulikakos [11] studied the effects of compression and pore size variations on the liquid flow characteristics in metal foams while Calmidi and co-workers [12, 13] suggested two models for the pore diameter evaluation as a function of porosity, pore diameter and shape function.

Vafai et al. [14] studied an empirical model where reference was made to an isotropic medium and the dependence on parameters, such as the geometric dimensions and the effective thermal conductivity, was accounted for. On the contrary, the variation of thermophysical properties with temperature was neglected, neither the inter- and intra-particle radiation heat transfer was taken into account, because of the rather low operating temperature.

Bhattacharya et al. [15] set up a model for the tortuosity, which improved the analytical results of the pressure gradient model proposed by Du Plessis et al. [16] by increasing the porosity limit of applicability.

Xu et al. [17] applied the heat and mass transfer steady models of porous media to solar receivers. They chose the volume convection heat transfer coefficient model, solved the equations numerically and analyzed the typical effect of porosity, average particle diameter, air inlet velocity and thickness on the temperature distribution.

Haussener et al. [18] used a tomography-based technique to characterize geometrical and thermophysical properties of reticulate porous ceramics, measuring porosity, surface area per unit of volume, mean pore size, permeability, and tortuosity. Also Petrasch et al. [19] used a computer tomography based methodology to determine the transfer characteristics of fluid flow across porous media. A 3-D digital representation of a Reticulate Porous Ceramic sample was generated by X-ray tomographic scans.

In this work a conjugate discrete model useful for the study and the simulation of heat transfer in a ceramic or metallic foam is presented, since, in literature there are no studies that combine laminar flow and radiative heat transfer. A Generation-based Technique is used for the foam representation, using the Weaire-Phelan structure [20] and all heat transfer mechanisms are taken into account and are studied using the COMSOL® Multiphysics.

2. Physics and mathematical description

The Generation-based Technique was used in the present study for the three-dimensional representation of the discrete structure of the foam. The geometrical model is based on the Weaire-Phelan foam structure, that is an evolution of the simpler tetradecahedron introduced by Lord Kelvin [21]. The computational domain is made up by a single cell and a fictitious inlet region useful to make negligible the lead effects, as shown in fig. 1. The single cell consists of the solid phase (green area) and of the fluid (blue area), that, generally, is air.

The main assumptions behind the mathematical model are steady-state, incompressible flow, homogeneous and constant properties gaseous and solid phases, grey body solid surfaces. The gaseous and solid phases can be at different temperatures and the local thermal non-equilibrium equations (LTNE) are used.

2.1 Fluid phase mathematical model

The single-phase fluid flow model equations used in the analysis of the fluid phase are presented in the following.

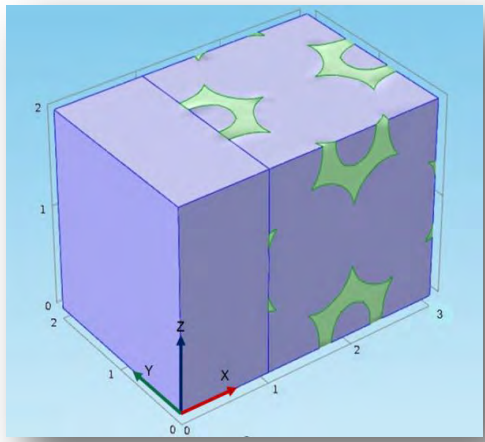

Figure 1. The complete structure imported into COMSOL® Multiphysics.

Continuity equation

$$\nabla \cdot \boldsymbol{u} = 0 \quad (1)$$

where $\boldsymbol{u}$ is the velocity vector.
Momentum equation

$$\rho\,(\boldsymbol{u}\cdot\nabla)\boldsymbol{u} = \nabla[-p + \mu\,(\nabla\boldsymbol{u} + (\nabla\boldsymbol{u})^T)] + \boldsymbol{F} \quad (2)$$

Energy equation

$$\rho\, C_p\, \boldsymbol{u}\cdot\nabla T_f = \nabla\cdot(k_f\,\nabla T_f) \quad (3)$$

The chosen coordinate system is shown in fig 1. Boundary conditions of the overall conjugated system depend on whether the solid structure or the fluid volume is considered.

The fluid structure is inscribed in a 2 mm ·2 mm · 2 mm cubic volume and the boundary conditions are

Wall No-Slip condition (*Fluid-to-Solid interface*)

$$\boldsymbol{u} = 0 \quad (4)$$

Continuity of heat flux (*Fluid-to-Solid interface*)

$$-\boldsymbol{n}\cdot\left(-k_f\,\nabla T_f\right) = -\boldsymbol{n}\cdot(k_s\,\nabla T_s) \quad (5)$$

Inflow condition (*Inlet surface: X = 0 mm*). In order to prescribe an inlet velocity profile, this boundary condition adds a weak contribution corresponding to the one-dimensional Navier-Stokes equation projected on the boundary. This condition assumes a plug flow in the fictitious inlet region

$$\boldsymbol{u} = -U_0\,\boldsymbol{n} \quad (6)$$

where U_0 is the modulus of the inflow velocity.

Temperature inflow condition (*Inlet surface: X = 0 mm*)

$$T = T_0 \quad (7)$$

with T_0 = 293.15 K.

Fluid interface condition (*Y = 0 mm; Y = 2 mm; Z = 0 mm; Z = 2 mm*). The slip condition assumes that there are no viscous effects at the fluid interface and, hence, no boundary layer develops. As to the model, this may be a reasonably accurate approximation, provided that the fluid does not leave the domain. Mathematically, the constraint can be formulated as

$$\boldsymbol{u}\cdot\boldsymbol{n} = 0,\ \ \boldsymbol{t}\cdot\left(-p + \mu(\nabla u + (\nabla u)^T)\right)\boldsymbol{n} = 0 \quad (8)$$

where $\boldsymbol{t}$ is a vector tangential to the boundary.

Symmetry condition (*X = 0 mm; X = 2 mm; Z = 0 mm; Z = 2 mm*)

$$-\boldsymbol{n}\cdot\left(-k_f\,\nabla T_f\right) = 0 \quad (9)$$

Outlet condition (*Outlet surface: X = 3 mm*). This boundary condition is physically equivalent to the flow entering a large container. The incompressible formulation of this boundary condition specifies a vanishing viscous stress along with a Dirichlet condition on the pressure

$$\mu(\nabla u + (\nabla u)^T)\boldsymbol{n} = 0, \qquad p = p_0 \quad (10)$$

where p_0 = 101,325 Pa.

Temperature outflow condition (*Plane X = 32 mm*)

$$-\boldsymbol{n}\cdot\left(-k_f\,\nabla T_f\right) = 0 \quad (11)$$

2.2 Solid phase mathematical model

As to the study of the solid phase, the mathematical model is based on the energy equation

$$\nabla\cdot(k_s\,\nabla T_s) = 0 \quad (12)$$

The solid is considered complementary to the fluid volume, inscribed in the same 2 mm ·2 mm · 2 mm cubic volume. Referring to the same coordinate system reported in fig 1, the boundary conditions are

Surface-to-surface radiation (*Solid-to-Fluid interface*)

$$-\boldsymbol{n}\cdot(-k_s\,\nabla T_s) = \varepsilon(I - \sigma T^4) - \boldsymbol{n}\cdot\left(k_f\,\nabla T_f\right) \quad (13)$$

where I is the incident radiation heat flux.

Prescribed radiosity (*X = 0 mm; Y = 0 mm and 0 mm ≤ X ≤ 1 mm; Y = 2 mm and 0 mm ≤ X ≤ 1 mm; Z = 0 mm and 0 mm ≤ X ≤ 1 mm; Z = 2 mm and 0 mm ≤ X ≤ 1 mm*)

$$J = I \quad (14)$$

Reradiating surface (*Trails of the fluid on planes Y = 0 mm; Z = 0 mm; Y = 2 mm; Z = 2 mm, with 1 mm ≤ X ≤ 3 mm*)

$$I = E \quad (15)$$

where E is the hemispherical emissive power.

The reradiating surface is a common approximation of a surface that is well

insulated on one side and for which convection effects can be neglected on the opposite radiating side.

Symmetry (*Trails of the solid structure on planes Y = 0 mm; Z = 0 mm; Y = 2 mm; Z = 2 mm, with* $(0\ mm \leq X \leq 2\ mm)$

$$-\boldsymbol{n} \cdot (-k_s \nabla T_s) = 0 \qquad (16)$$

3. Numerical analysis

The procedure from cell modeling to the final flow solving consists of the following steps

- development of the three-dimensional cell structure,
- implementation of the mesh based on the geometry built before,
- flow and heat solving using COMSOL Multiphysics®.

The foam geometry developed by Phelan et al. [20] is defined in an input file in the free-to-use "Surface Evolver" surface energy minimization software, as described in Brakke [22]. A fluid phase is added to the foam using the same software. The virtual surface tension and porosity of the final foam are adjusted by changing specified parameters and, after refinements and iterative processes, a single representative cell of the foam is cut, fitting a virtual bounding box. The open faces of the cell are then capped to obtain a closed structure.

The closed mesh structure obtained is exported in STL format. It is then imported into COMSOL® as geometry. A careful manual choice of face partitioning parameters allows COMSOL® to correctly recognize and mesh the solid domain.

To define the fluid domain, a box enclosing the entire solid structure is created firstly, then a boundary-preserving boolean union with the solid structure is performed, obtaining two separate but contacting solid and fluid domains. Finally, COMSOL®'s own meshing utilities are used to define 3D-meshes of both domains: a boundary layer mesh for the fluid structure and a free tetrahedral mesh for the solid one (fig.2). Here, the appropriate boundary conditions are defined, along with the fluid properties, and the problem is solved.

The built-in module of COMSOL® Conjugate Heat Transfer is used for the resolution of the problem. It provides the combined use of Heat Transfer in Solids and Flow modulus within the structure. The radiative heat transfer is simulated considering

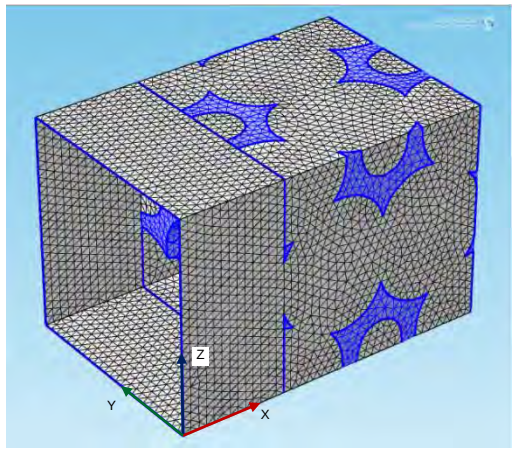

Figure 2. Mesh of the structure

a Surface-to-Surface radiation model. It calculates view factors by means of the hemicube method. Preliminary tests allowed to assume the flow to be laminar.

4. Results and Discussion

The present study was carried out considering a 92.5% cell porosity, the Weaire-Phelan foam structure inscribed in a 2 mm · 2 · mm · 2 mm cubic volume, a 2 m/s U_0 input velocity a 7.5 · 10^5 W/m^2 incident radiation heat flux and a 0 Pa outlet pressure. It was, therefore, possible to analyze the behavior of the material undergoing a conjugate heat transfer that takes also into account pressure drops inside the structure. Reference being made to a ceramic material (SiC) and air, respectively, the distribution of cell surface temperature (K), velocity (m/s) and pressure (Pa) has been calculated. Results are shown in figs. 3, 4 and 5, respectively.

Temperature (°C) and pressure (Pa) fields

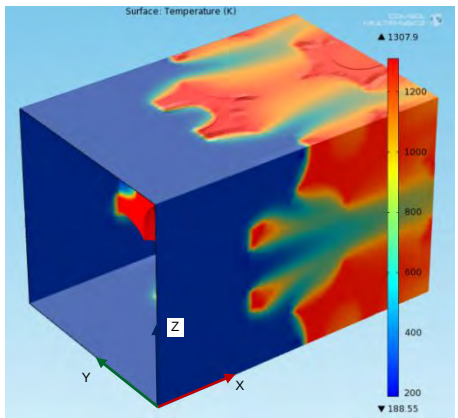

Figure 3. Distribution of the cell surface temperature (K).

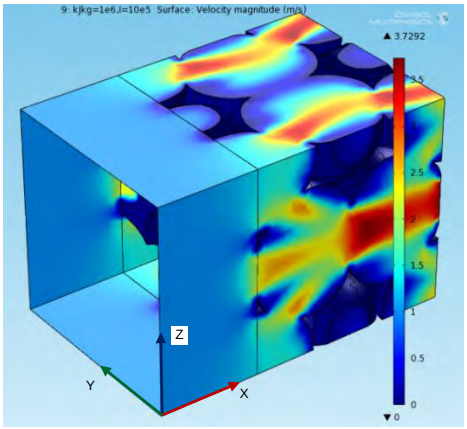

Figure 4 Distribution of the cell surface velocity (m/s).

in planes $Y = 1$ mm (a) and $Z = 1$ mm (b) are reported in figs. 6 and 7, respectively.

Figure 6 shows that higher temperatures are attained in the solid phase than in the fluid one. The foam solid structure is heated by the incident radiation on the $X = 0$ mm plane, and heat is then transferred to the remaining solid structure mainly by conduction and radiation. The temperature of the solid structure temperature varies in 1,200 K - 1,300 K range. The temperature of the fluid increases because of convective heat transfer with the solid phase and a nearly 1,000 K fluid outlet temperature is attained.

Figure 7 exhibits a pressure drop of about 10 Pa in the 2.0 mm long unit cell. One can also notice that pressure decreases near solid edges, where the cross section available to the fluid diminishes. On the contrary, pressure increases in proximity of solid edges where a stagnation of the fluid occurs.

Velocity (m/s) fields in planes $Y = 1$ mm (a) and $Z = 1$ mm (b) are presented in figs. 8.

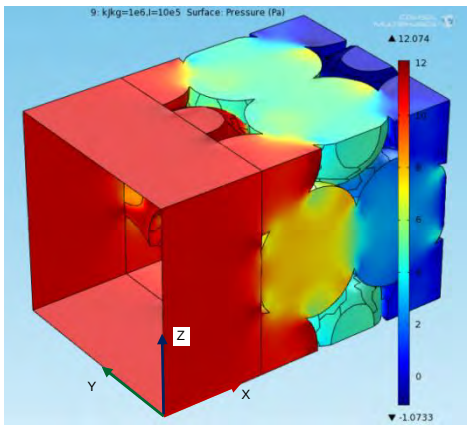

Figure 5. Distribution of the cell surface pressure (Pa).

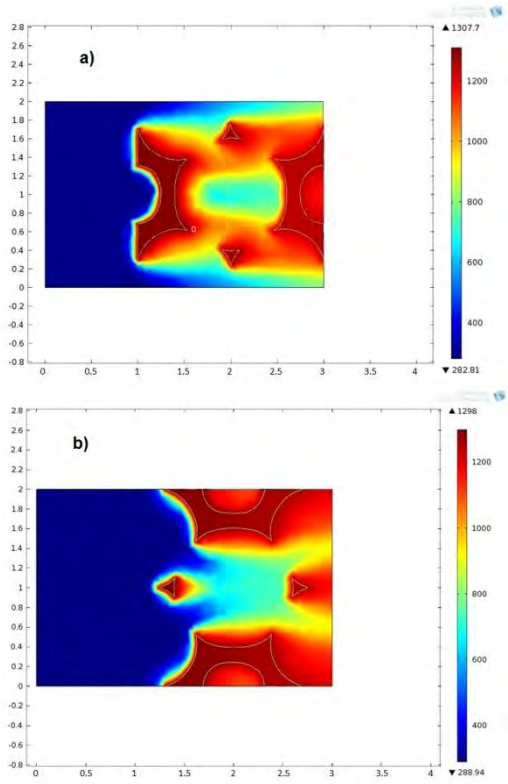

Figure 6. Temperature (K) fields: a) $Y = 1$ mm; b) $Z = 1$ mm.

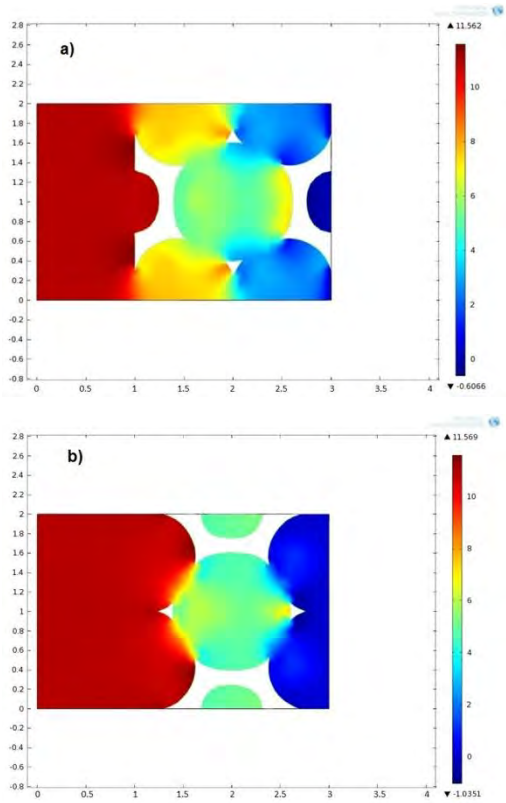

Figure 7. Pressure (Pa) fields: a) $Y = 1$ mm; b) $Z = 1$ mm.

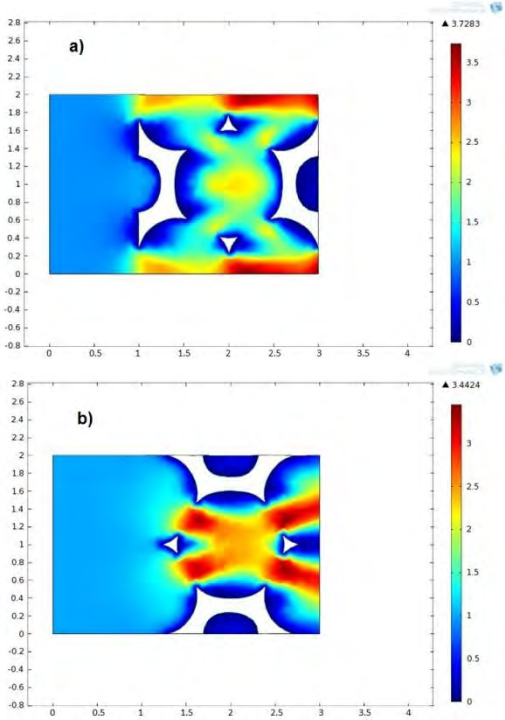

Figure 8. Velocity (m/s) fields: a) $Y = 1$ mm; b) $Z = 1$ mm.

Stagnation zones can be observed both upstream and downstream of solid parts, whereas velocity magnitude is larger where the flow cross section decreases.

The above presented results allow the evaluation of coefficients to be employed in continuous models of the foam. The use of a continuous representation enables the study of more complex problems, thanks to computational costs that are more affordable than those for discrete modelling.

5. Conclusions

Conjugate conductive-convective-radiative heat transfer in an air saturated SiC ceramic foams was analyzed. A Representative Elementary Volume of the foam, based on the Weaire-Phelan structure, was obtained by the Surface Evolver code. A single Weaire-Phelan cell was imported in COMSOL® Multiphysics. It was meshed and pressure, velocity and temperature fields were obtained by solving the conjugate heat transfer problem.

Results from these simulations were useful to evaluate coefficients to be employed in continuous models of the foam.

The continuous approach could be applied to the study of different applications, such as high-temperature solar power plants and electric or thermal insulation, where a discrete representation of the foam required unsustainable computational costs.

6. Nomenclature

C_p	specific heat	J/kg K
E	hemispherical emissive power	W/m^2
$\boldsymbol{F}$	body force	N/m^2
I	incident radiation heat flux	W/m^2
J	radiosity	W/m^2
k	thermal conductivity	W/m K
$\boldsymbol{n}$	normal to a surface	
p	pressure	Pa
$\boldsymbol{u}$	velocity	m/s
U	modulus of the inflow velocity	m/s
$\boldsymbol{t}$	tangential to a surface	
T	temperature	K
x, y, z	Cartesian coordinates	m
Greek symbols		
ε	emissivity	
ρ	density	kg/m^3
σ	Stephan-Boltzmann constant	W/m^2K^4
Subscripts		
f	fluid	
s	solid	
0	inlet surface	

7. References

1. Z. Wu, C. Caliot, G. Flamant, Z. Wang, Coupled radiation and flow modelling in ceramic foam volumetric solar air receivers, *Solar Energy*, **85**, 2374-2385 (2011).

2. T. James, *Energy and emissions markets: Collision or convergence,* Wiley&Sons, Asia (2011).

3. Q. Pang, G.H. Wu, Z.Y. Xiu, G.Q. Chen, D.L. Sun, Synthesis and mechanical properties of open-cell Ni–Fe–Cr foams, *Materials Science and Engineering:A*, **534**, 699-706 (2012).

4. P.T. Garrity, F.J. Klausner, R. Mei, Performance of aluminum and carbon foams for air side heat transfer augmentation, *ASME J. Heat Transfer*, **132**, 121901-121910 (2010).

5. D.Y. Lee, K. Vafai, Analytical characterization and conceptual assessment of solid and fluid temperature differentials in porous media, *Int. J. Heat Mass Transfer*, **Vol. 42**, 423-435 (1999).

6. D. Angirasa Forced convective heat transfer in metallic fibrous materials, *ASME J. Heat Transfer*, **Vol. 124**, 739-745 (2002).

7. D. Poulikakos, K. Renden, Forced convection in a channel filled with porous medium, including the effect of flow inertia, variable porosity and Brinkman friction, ASME J. Heat Transfer, **109**, 880-888 (1987).
8. D. Poulikakos, M. Kazmierczak, Forced convection in a duct partially filled with a porous material, *ASME J. Heat Transfer*, **Vol. 109**, 653-662 (1987).
9. H.R. Seyf, M. Layeghi, Numerical Analysis of convective heat transfer from elliptic pin fin heat sink with and without metal foam insert, *ASME J. Heat Transfer*, **132**, 1-9 (2010).
10. M. Gan, J. Wang, *Advanced Image Acquisition, Processing Techniques and Applications,* 109-122. InTech, UK (2009).
11. K. Boomsma, D. Poulikakos, The effects of compression and pore size variations on the liquid flow characteristics in metal foams, J. *Fluid Engineering*, **124**, 263-272 (2002).
12. V.V. Calmidi, R.L. Mahajan, Forced convection in high porosity metal foams, *ASME J. Heat Transfer*, **122**, 557-565 (2000).
13. V.V. Calmidi, Transport phenomena in high porosity fibrous metal foams, *Ph.D. thesis*, University of Colorado, Boulder, CO (1998).
14. K. Vafai, A. Amiri, Analysis of dispersion effects and non-thermal equilibrium, non-Darcian, variable porosity incompressible flow through porous media, *Int. J. Heat Transfer*, **37**, 939-954 (1994).
15. A. Bhattacharya, V.V. Calmidi, R.L. Mahajan, Thermophysical properties of high porosity metal foams, *Int. J. Heat Mass Transfer*, **45**, 1017-1031 (2002).
16. P. Du Plessis, A. Montillet, J.C. Comiti, J. Legrand, Pressure drop prediction for flow through high porosity metallic foams, Chem. Eng. Sci., **49**, 3545–3553 (1994).
17. C. Xu, Z. Song, L. Chen, Y. Zhen, Numerical investigation on porous media heat transfer in a solar tower receiver, *Renewable Energy*, **36**, 1138-1144 (2011).
18. S. Haussener, P. Coray, W. Lipinski, P. Wyss, A. Steinfeld, Tomography-based heat and mass transfer characterization of reticulate porous ceramics for high-temperature processing, *ASME J. Heat Transfer*, **132**, 1-9 (2010).
19. J. Petrasch, F. Meier, H. Friess, A. Steinfield, Tomography based determination of permeability, Dupuit-Forchheimer coefficient, and interfacial heat transfer coefficient in reticulate porous ceramics, *Int. J. Heat and Fluid Flow*, **29**, 315-326 (2008).
20. R. Phelan, D. Weaire, E.A.J.F. Petres, The conductivity of a foam, *Journal of Physics: Condensed Matter*, **8**, 475-482 (1996).
21. Lord Kelvin, On the division of space with minimum partitional area, *Philosophical Magazin*, **24**, 503-514 (1887).
22. K.A. Brakke, The surface evolver, *Experimental Mathematics*, **1**, 141-165, (1992).

8. Acknowledgements

This work was carried out within an Agreement between the University of Connecticut and the Università di Napoli Federico II and was supported by Italian Government MIUR grant PRIN-2009KSSKL3.